

## A Record Anisotropy Barrier for a Single-Molecule Magnet

Constantinos J. Milios,<sup>†</sup> Alina Vinslava,<sup>‡</sup> Wolfgang Wernsdorfer,<sup>§</sup> Stephen Moggach,<sup>†</sup>  
Simon Parsons,<sup>†</sup> Spyros P. Perlepes,<sup>||</sup> George Christou,<sup>‡</sup> and Euan K. Brechin\*<sup>†</sup>*School of Chemistry, The University of Edinburgh, West Mains Road, Edinburgh, EH9 3JJ, U.K., Laboratoire Louis Néel-CNRS, 38042 Grenoble, Cedex 9, France, Department of Chemistry, University of Florida, Gainesville, Florida 32611-7200, Department of Chemistry, University of Patras, 26504 Patras, Greece*

Received December 14, 2006; E-mail: ebrechin@staffmail.ed.ac.uk

Magnets have fascinated humans for millenia, playing a prominent role in the development of modern society, science, and technology, and making up a multi-billion-dollar-per-year industry. Classical or atom-based magnets, for example, metals, metal alloys, and metal oxides, are composed solely of a high density of d- or f-orbital metal spin sites and are prepared by high-temperature metallurgical methods. The development of molecule-based magnets<sup>1</sup> enabled the specific alteration of the magnetic properties by established organic or coordination chemistry techniques and the combination of magnetic properties with other mechanical, electrical and/or optical properties in harmony with simplicity of fabrication.<sup>2,3</sup> Current trends in the research field of molecular magnetism mainly involve activities in three classes of molecular materials, namely, multifunctional magnetic materials, nanostructured magnetic materials, and molecular nanomagnets.<sup>4</sup> As far as molecular nanomagnets are concerned, the past few years have witnessed an explosive growth in the interest in single-molecule magnets (SMMs).<sup>5</sup> The first and still best studied SMMs are the mixed-valent  $[\text{Mn}_{12}\text{O}_{12}(\text{O}_2\text{-CR})_{16}(\text{H}_2\text{O})_4]$  ( $\text{Mn}_{12}$ ; R = various) family with an  $S = 10$  ground state, which are the SMMs with the highest blocking temperatures ( $T_B \approx 3.5$  K) and  $U_{\text{eff}}$  values (up to 74 K).<sup>6</sup> The first example of a  $\text{Mn}_{12}$  SMM was the R=Me derivative  $[\text{Mn}_{12}\text{O}_{12}(\text{O}_2\text{CMe})_{16}(\text{H}_2\text{O})_4] \cdot 2\text{MeCO}_2\text{H} \cdot 4\text{H}_2\text{O}$  ( $\text{Mn}_{12}\text{OAc}$ ) with  $D = -0.72$  K ( $-0.50$   $\text{cm}^{-1}$ ),  $U = 72$  K ( $50$   $\text{cm}^{-1}$ ), and  $U_{\text{eff}} = 60\text{--}64$  K. After almost a decade and a half of intense research in this area, complex  $\text{Mn}_{12}\text{-OAc}$  and its carboxylate-substituted derivatives still remain the molecules that can function as magnets at the highest temperatures. This is despite the preparation of many SMMs of different structural types.<sup>5</sup> Herein we demonstrate that the deliberate use of bulky organic bridging ligands that can cause targeted structural distortions to the cores of (known) polymetallic cluster complexes can provide a new pathway toward obtaining high-spin molecules with enhanced blocking temperatures. Specifically we show that the deliberate structural distortion of the core of the hexametallate complex  $[\text{Mn}^{\text{III}}_6\text{O}_2(\text{sao})_6(\text{O}_2\text{CPh})_2(\text{EtOH})_4]$  ( $\text{saoH}_2 = \text{salicylaldehyde oxime}$  or 2-hydroxybenzaldehyde oxime) switches the dominant magnetic exchange interactions among metal centers from antiferromagnetic to ferromagnetic resulting in a molecule with  $S = 12$  and  $D = -0.43$   $\text{cm}^{-1}$  in the ground state and an effective energy barrier to magnetization reversal of 86.4 K,  $\sim 12$  to 13 K higher than that of the  $\text{Mn}_{12}$  family.

The complex  $[\text{Mn}^{\text{III}}_6\text{O}_2(\text{sao})_6(\text{O}_2\text{CPh})_2(\text{EtOH})_4]$  (**1**) is characterized by an  $S = 4$  spin ground state as a result of the ferromagnetic exchange between two antiferromagnetically coupled  $[\text{Mn}^{\text{III}}_3]$  triangles.<sup>7</sup> We previously showed that when the  $\text{sao}^{2-}$  bridging ligands are deliberately replaced with their larger, bulkier derivative

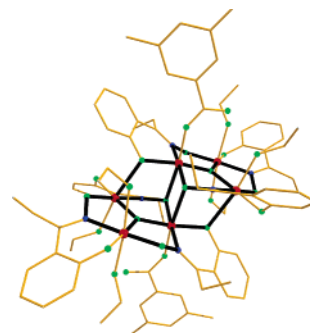


**Figure 1.** The molecular structure of **3** with the central core highlighted in black. Color code: Mn, red; O, green; N, blue.

$\text{Et-sao}^{2-}$  ( $\text{Et-saoH}_2 = 2\text{-hydroxyphenylpropanone oxime}$ ) to give the analogous complex  $[\text{Mn}^{\text{III}}_6\text{O}_2(\text{Et-sao})_6(\text{O}_2\text{CPh})_2(\text{EtOH})_6]$  (**2**) there occurs a significant structural modification of the core of the complex—a severe twisting of the Mn–N–O–Mn moieties (i.e., the oximate linkage) within each  $[\text{Mn}_3]$  subunit and a change in the binding mode of the carboxylate from  $\mu$ -bridging to monodentate, which results in a switch in the dominant magnetic exchange interactions from antiferromagnetic to ferromagnetic and thus the stabilization of an  $S = 12$  ground state in **2**.<sup>8</sup> However, the weak exchange (approximately  $+0.90$   $\text{cm}^{-1}$ ) present in **2** results in the population of low-lying excited states, and tunneling involving excited-state multiplets gives rise to a dramatic reduction in the energy barrier to magnetization relaxation from a theoretical upper limit of 89 K to an effective barrier  $U_{\text{eff}} = \sim 53$  K.<sup>8</sup> Replacement of the benzoate in **2** with 3,5-dimethylbenzoate via a simple metathesis type reaction produces the analogous complex  $[\text{Mn}^{\text{III}}_6\text{O}_2(\text{Et-sao})_6(\text{O}_2\text{CPh}(\text{Me})_2)_2(\text{EtOH})_6]$  (**3**, Figure 1). The core of **3** is identical to that seen for **2**, except that the Mn–N–O–Mn torsion angles have increased still further from an average of  $\alpha_v = 36.5^\circ$  in **2** to  $\alpha_v = 39.1^\circ$  in **3**. A comparison of the susceptibility data (Figure 2) shows that the exchange in **3** appears to be somewhat stronger, with a simulation of the data assuming a simple one- $J$  model (see Supporting Information for details) suggesting an almost 2-fold increase from  $J = +0.9$   $\text{cm}^{-1}$  in **2** to  $J = +1.6$   $\text{cm}^{-1}$  in **3**. Magnetization data for **3** (Figure 2) obtained at low temperatures and high fields confirm the  $S = 12$  ground state, with  $g = 1.99$  and  $D = -0.43$   $\text{cm}^{-1}$ . These parameters are consistent with those observed for **2** and suggest a barrier for magnetization reorientation with an upper limit of  $S^2|D| = 89$  K. For powdered microcrystalline samples of complex **3**, fully visible, frequency-dependent out-of-phase ( $\chi''_M$ ) ac susceptibility signals are seen below  $\sim 10$  K with the peak at 1500 Hz occurring at  $\sim 7$  K (Figure 3). These data afford an energy barrier to magnetization relaxation of 86.4 K. Confirmation of the barrier height comes from combining this data with that obtained from single-crystal dc relaxation measurements performed

<sup>†</sup> University of Edinburgh.<sup>‡</sup> University of Florida.<sup>§</sup> Laboratoire Louis Néel-CNRS.<sup>||</sup> University of Patras.

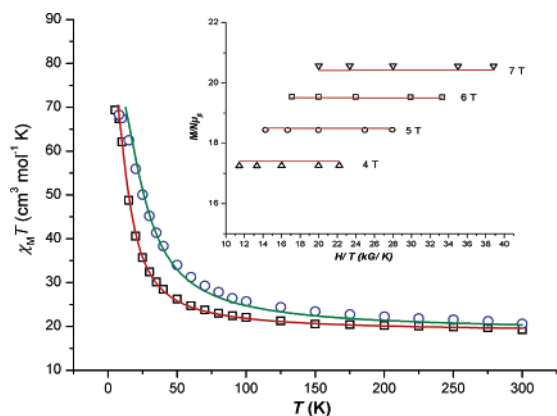


**Figure 2.** Plot of  $\chi_M T$  vs  $T$  for complexes **2** ( $\square$ ) and **3** ( $\circ$ ). The solid lines represent simulations of the experimental data in the temperature range 300–5 K. The inset is a plot of reduced magnetization ( $M/N\mu_B$ ) versus  $H/T$  for **3** in the field and temperature ranges 4–7 T and 2–6 K. The solid lines correspond to the fit of the data. See text and SI for details.

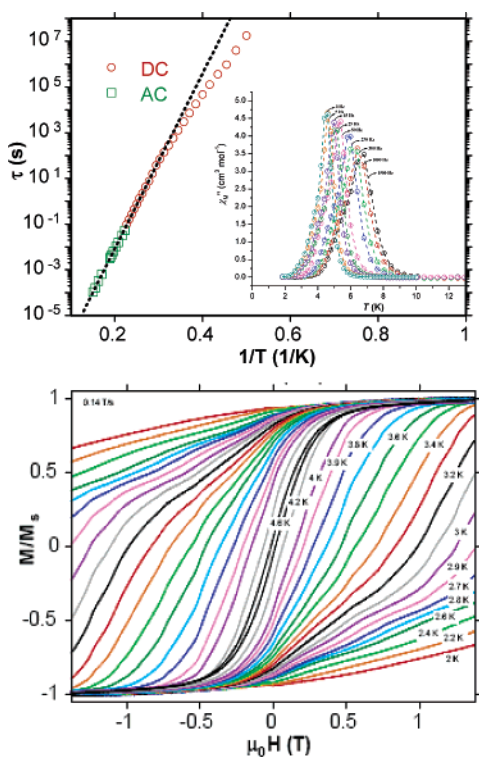


**Figure 3.** (top) Arrhenius plot using ac (green) and dc (red) data. The dashed line is the fit of the thermally activated region; (inset) out-of-phase ( $\chi_M''$ ) ac susceptibility measurements in the 1.8–12 K and 50–1500 Hz ranges. The bottom panel shows the magnetization versus field hysteresis loops for a single crystal of **3** at the indicated temperatures in a field sweep rate of 0.14 T s $^{-1}$ .  $M$  is normalized to its saturation value.

on a micro-SQUID.<sup>9</sup> Above approximately 2 K the relaxation rate is temperature-dependent with the fits yielding  $U_{\text{eff}} = 86.4$  K with  $\tau_0 = 2 \times 10^{-10}$  s (Figure 3). Below 2 K however, the relaxation rate becomes of the order of several months, and its rate becomes difficult to accurately determine. The relaxation can be increased

by applying a field opposite to the magnetization direction—this is done in hysteresis loop measurements (Figure 3) where the hysteresis between a sweep from positive to negative field and back indicates that the magnetization relaxes slower than the time scale given by the field sweep rate. Single-crystal hysteresis loops indicate an opening of the loops at a temperature of  $\sim 4$  K at a sweep rate of 1 mT s $^{-1}$ . The hysteresis increases continuously for lower temperatures and reaches a maximum at about 0.6 K (Figure SI2). Below this temperature the loops become temperature independent. This behavior, in addition to the steplike structure of the loops, indicates resonant quantum tunneling between energy levels of the spin system. Such behavior has already been well studied for other SMMs. The important point here is that the single-crystal studies demonstrate that the relaxation of **3** is much slower than that of **2** and approximately *ten times* slower than that of Mn<sub>12</sub>–BrAc—which had, until now, the highest barrier.<sup>6</sup>

In conclusion, the deliberate structural distortion of a known [Mn<sub>6</sub>] molecule switches the dominant magnetic exchange from antiferromagnetic to ferromagnetic resulting in a molecule possessing an  $S = 12$  ground state with  $D = -0.43$  cm $^{-1}$ . Relaxation studies on both powdered samples and on single crystals reveal the complex to be a single-molecule magnet with a record value of the effective energy barrier to magnetization reversal ( $U_{\text{eff}}$ ) of 86.4 K and a blocking temperature of  $\sim 4.5$  K, finally breaking the long-standing record held by the Mn<sub>12</sub> family of molecules. The result suggests that intelligent, targeted structural distortion can be a powerful new tool in the design of molecules with greatly enhanced blocking temperatures. This work emphasizes the importance of obtaining synthetic control over obtained SMMs, so that they can be modified in desirable ways. This thus allows expansion of a particular structural type into a family of related species that are invaluable in probing the various factors that affect the observed magnetic properties. We are optimistic that SMMs with even higher blocking temperatures and slower relaxation rates will be amenable to synthesis.

**Acknowledgment.** This work was supported by the Leverhulme Trust and EPSRC (U.K.), the NSF and PYTHAGORAS I (Greece).

**Supporting Information Available:** Crystallographic details in cif format, synthetic procedures and magnetism data. This material is available free of charge via the Internet at <http://pubs.acs.org>.

## References

- (1) Kahn, O. *Acc. Chem. Res.* **2000**, *33*, 647–657.
- (2) Miller, J. S.; Epstein, A. J. *Angew. Chem., Int. Ed. Engl.* **1994**, *33*, 385–415.
- (3) Miller, J. S.; Epstein, A. J. *Chem. Br.* **1994**, 477–480.
- (4) Coronado, E.; Gatteschi, D. *J. Mater. Chem.* **2006**, *16*, 2513–2515.
- (5) Aromí, G.; Brechin, E. K. *Struct. Bonding* **2006**, *122*, 1–67. Christou, G.; Gatteschi, D.; Hendrickson, D. N.; Sessoli, R. *MRS Bull.* **2000**, *25*, 66–71. Gatteschi, D., Sessoli, R. *Angew. Chem., Int. Ed.* **2003**, *42*, 268–297.
- (6) Chakov, N. E.; Lee, S.-C.; Harter, A. G.; Kuhns, P. L.; Reyes, A. P.; Hill, S. O.; Dalal, N. S.; Wernsdorfer, W.; Abboud, K.; Christou, G. *J. Am. Chem. Soc.* **2006**, *128*, 6975–6989.
- (7) Milios, C. J.; Raptopoulou, C. P.; Terzis, A.; Lloret, F.; Vicente, R.; Perlepes, S. P.; Escuer, A. *Angew. Chem., Int. Ed.* **2003**, *43*, 210.
- (8) Milios, C. J.; Vinslava, A.; Wood, P. A.; Parsons, S.; Wernsdorfer, W.; Christou, G.; Perlepes, S. P.; Brechin, e. K. *J. Am. Chem. Soc.* **2007**, *129*, 8–9.
- (9) Wernsdorfer, W. *Adv. Chem. Phys.* **2001**, *118*, 99.

JA068961M